ACOUSTICS 2017 PERTH
SOUND, SCIENCE AND SOCIETY

Propagation of underwater noise from an offshore seismic survey in Australia to Antarctica: measurements and modelling

Alexander Gavrilov (1)

(1) Centre for Marine Science and Technology, Curtin University, Perth, Australia

ABSTRACT

An offshore seismic survey was conducted over the western edge of the continental shelf in Bass Strait in 2006. Underwater noise from this survey was recorded on an autonomous sound recorder deployed in the Southern Ocean on the Antarctic continental slope. Sound emission and propagation models were verified by experimental measurements based on parameters and position of the airgun array and characteristics of the underwater sound channel. A parabolic equation approximation method was used to calculate the sound field over the continental slope of Australia and then a normal mode model was employed to account for the transmission loss due to sound scattering by surface waves south of the Polar front. The numerical predictions are consistent with the measurement results within a few dBs for the sound exposure and energy spectral levels. It is also demonstrated by measurements and modelling that the best coupling of a near-surface sound source with the SOFAR underwater sound channel takes place when the source is located over the continental slope at a sea depth of about half of the channel's axis depth. The model can be used to predict masking effects of man-made underwater noise on the communication environment of marine mammals in Antarctica.

1 INTRODUCTION

An offshore seismic survey, termed Aragorn, was conducted by PGS Geophysical over the western edge of the continental shelf in Bass Strait in April-May 2006. Details of this survey related to characteristics and position of the airgun array used in the survey and a description of underwater noise measurements made at the same time using three autonomous underwater noise recorders in the Southern Ocean (Figure 1) are provided in Gavrilov *et al*., 2016. In this paper, a numerical approach is presented to model sound emission and propagation from the airgun array to the furthermost underwater sound recorder deployed on the continental slope in Antarctica, at location 3 shown on the map in Figure. 1.

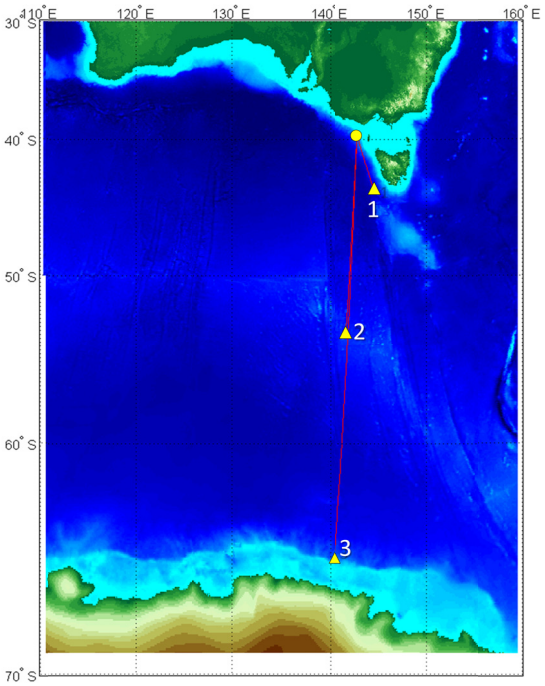

Figure 1: Locations of the underwater sound recorders deployed in the Southern Ocean in 2006 (red triangles), location of the Aragorn seismic survey (red circle) and the sound propagation paths (red lines).

A model of the sound signal emitted by the airgun array and the sound propagation model across the Southern Ocean are presented in the next section. Modelling results are compared with measurement data in Section 3.

2 MODELLING APPROACH

2.1 Source signal

The sound signal emitted by the airgun array was modelled using a numerical model of sound emission from single guns and airgun arrays developed at the Centre for Marine Science and Technology (CMST), Curtin University (Duncan, 1998). The model calculates the signal waveform in the far field, i.e. at a distance much larger than the array dimensions. Then the waveform amplitude is back-extrapolated to a distance of 1 m from the array geometrical centre using the spherical spreading law for the transmission loss, so that the array is modelled by a directional point source. As the array is a directional source of sound signal, the source signal waveform is modelled for different azimuth and elevation angles. The azimuth angle is commonly measured clockwise relative to the vessel/array heading, and the elevation angle is measured relative to the downward vertical direction, so that it is 90° for the horizontal emission. The input parameters of the model are the array geometry (as shown in Figure 4 in Gavrilov *et al*., 2016) and the volume and chamber pressure of each active gun in the array.

The heading direction of all seismic tracks of the survey was either about 30° or 330° relative to the direction of sound propagation to the recorder in Antarctica. Figure 2 shows the sound signal waveform emitted by the array at an azimuth angle of 330° and elevation angle of 90°.

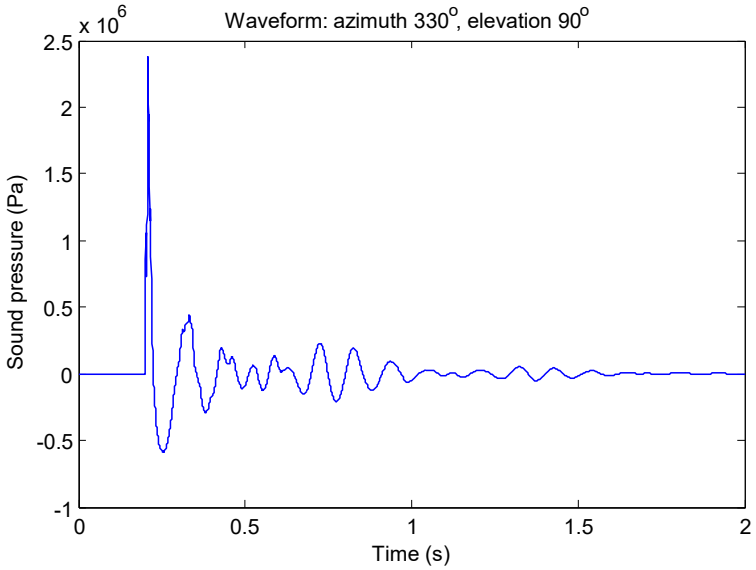

Figure 2: Sound signal waveform at 1 m from the airgun array centre, modelled for an azimuth angle of 330° and elevation angle of 90°.

The Energy Spectral Density (ESD) level of the sound signal emitted by the array at 330° is shown in Figure 3. It is averaged over the elevation angles from 45° to 90° where most of the sound energy is coupled with the underwater sound channel. Averaging over the elevation angle is applied to simplify calculations of the sound transmission loss with range, as most of the common sound propagation models do not directly accept point sources with vertical directionality. The ESD level decays from about 10 Hz to nearly 100 Hz. The broad peak at around 10 Hz is formed by the energy of air bubble pulsations which have slightly different frequencies for airguns with different volumes in the array. The modelled ESD shown in Figure 3 was used to predict the ESD at the sound receiver in Antarctica.

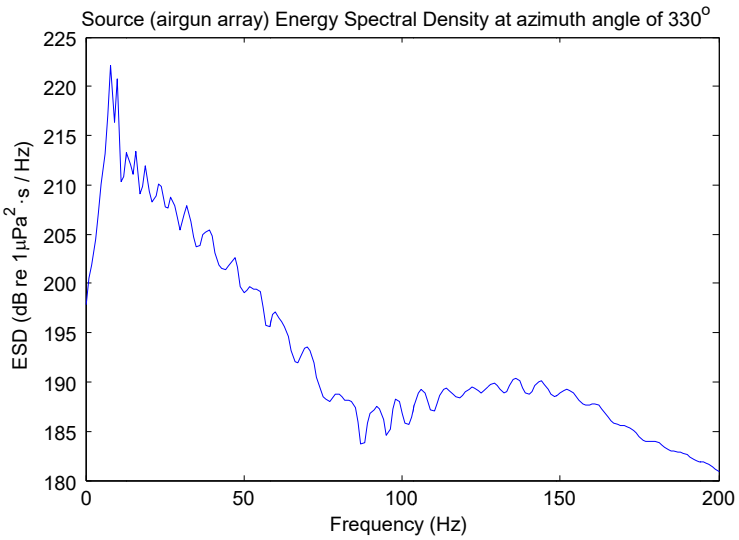

Figure 3: Energy spectral density level of the sound signal at 1 m from the airgun array centre at an azimuth angle of 330°, averaged for elevation angles from 45° to 90°.

2.2 Sound transmission model

The underwater sound transmission channel from Bass Strait to Antarctica is highly range dependent. Firstly, it lies over a steep continental slope of Australia. Secondly, it crosses a sharp Polar front at the Antarctic convergence, where the axis of the underwater sound channel ascends rapidly from about 1100 m depth to the sea surface (Figure 4). The bathymetry along the sound transmission path was modelled using the Geoscience Australia bathymetry and topography grid of 250 m resolution (http://www.ga.gov.au/metadata-gateway/metadata/record/gcat_67703) for the initial path section of 350 km length over the Australian continental slope and the ETOPO2 gridded bathymetry/topography data (https://www.ngdc.noaa.gov/mgg/fliers/01mgg04.html) for the following section of the path.

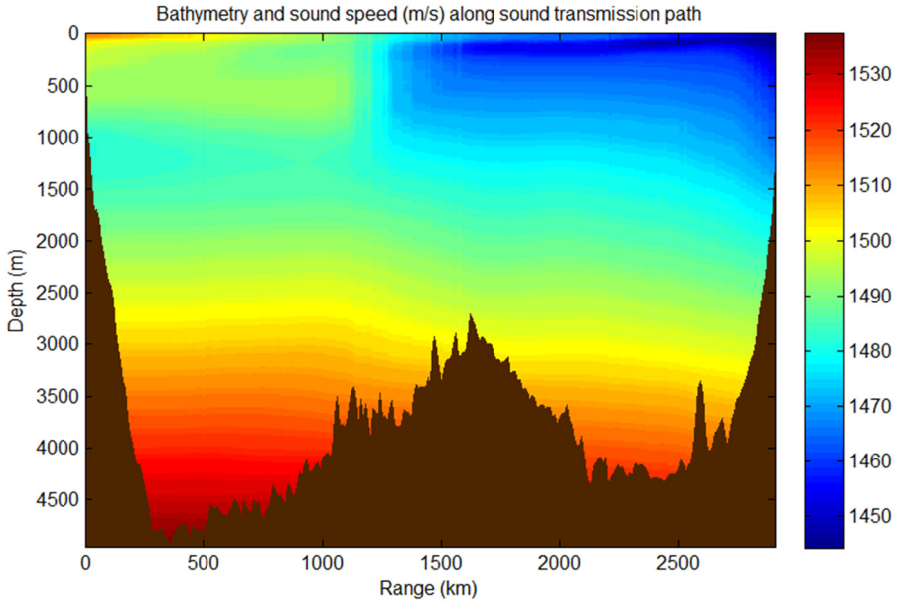

Figure 4: Bathymetry and sound speed profile along the sound transmission path from Bass Strait to the sound recorder in Antarctica.

The sound speed profile along the transmission path was modelled using the World Ocean Atlas gridded climatology data of 0.25° spatial resolution (https://www.nodc.noaa.gov/OC5/woa13/). Water temperature and salinity data for austral autumn were used to calculate the sound speed profiles.

The geoacoustic properties of the seabed along the sound transmission path were generally unknown. Results of numerical modelling (Section 3) showed that the sound interaction with the seafloor was significant only along

the transmission path sections over the continental slope in Australia and Antarctica. Based on a number of probes taken on the Australian continental slope at various locations, the seabed was assumed to be covered with medium to coarse sand. The sound speed in the seabed material was set in the model to be 1770 m/s, the density 1800 kg/m^3 and attenuation 0.47 dB/λ. As the seafloor properties over the continental slope in Antarctica were unknown, they were assumed to be similar to those near Australia, which might be an insufficiently accurate representation of the seafloor model.

The airgun array was towed at 6 m below the sea surface. Because it was essential to accurately model the coupling of a near-surface sound source with the deep sound channel in the temperate ocean south of Australia, a Parabolic Equation (PE) approximation method was chosen to model sound transmission from the airgun array over the initial section of the path of 350 km length lying over the continental slope. A coupled normal mode method would also be capable of modelling the coupling of near-surface source with the deep sound channel over the continental slope. However, it's computationally less efficient than the PE method in an underwater sound channel over rapidly changing bathymetry, where normal modes are to be calculated on a fine range grid.

The available PE computer models, including RAMGeo (http://cmst.curtin.edu.au/products/underwater/) used in this study, are incapable of accounting for the transmission loss due to scattering of sound waves by the surface wind waves, which is critical for the path section beyond the polar front. To include the scattering effect on the sound transmission loss, a normal mode approach was employed. The sound field predicted by the PE model at 350 km from the source was expanded into a series of local normal modes, as described in Wilkes et al. (2016). Then the modes were propagated over the rest of the transmission path to calculate the sound field and transmission loss at the sound receiver.

The normal modes were calculated using the computer normal mode model ORCA (Westwood *et al.*, 1996). As the mode coupling effect across the polar front was not expected to be significant, based on Li and Gavrilov (2006), an adiabatic mode approximation was employed, which made calculations much more computationally efficient. The surface scattering effect was modelled using the Kuperman-Ingenito boundary perturbation approximation, where the imaginary part of the modal wavenumber is increased by the scattering component:

$$\gamma_n^S = \frac{\sigma^2 \beta_n}{2k_n} Z_n'(0)^2 ,$$

where σ is the RMS height of surface waves, Z_n is the mode function (mode shape), k_n is the real part of mode wavenumber, $\beta_n = \sqrt{k^2 - k_n^2}$ is the vertical component of the wavenumber $k = 2\pi f / c$. The RMS height σ of surface roughness was assumed to be 2 m, which corresponds to a significant wave height of approximately 8 m typical for the high-latitude part of the Southern Ocean.

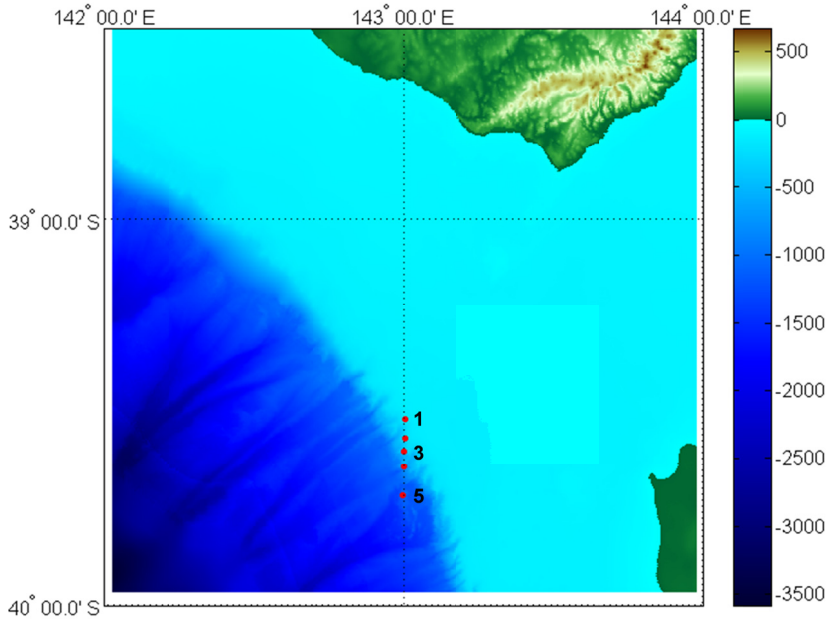

Figure 5: Five locations of the sound source assumed in the model.

The transmission loss was calculated in the frequency band from 5 Hz to 100 Hz with a 1 Hz increment. The modelling band was limited by those frequencies because: (1) the modelled source signal ESD drops steeply below 5 Hz and no airgun noise energy was observed below 5 Hz in the measurement data and (2) no energy of airgun signals was observed above approximately 50 Hz (see next section). The modelling band was extended to 100 Hz to assess the airgun noise spectrum at shallower receiver depths.

In the model, the sound source (airgun array) was placed at five different locations over the continental shelf and slope spanning the range of water depth variations in the area of the seismic survey. These locations are shown in Figure 5. The receiver was placed at 1100 m below the sea surface which was the depth of the sound recorder in the measurements.

3 MODELLING RESULTS AND COMPARISON WITH EXPERIMENTAL DATA

The top panel of Figure 6 shows a long-time average spectrogram of sea noise recorded over the time period of the major part of the seismic survey in May 2006. Periods with airgun noise can be recognised in this spectrogram by broadband noise of higher intensity from approximately 7 Hz to nearly 50 Hz. The bottom panel shows the sea depth at the source location at the times of airgun discharge, which was taken from the p1/90 data record provided by PGS. The airgun noise could not be distinguished in the background noise when the seismic vessel operated over the shelf in shallower water of less than 150 m sea depth. It also can be concluded from this figure that the intensity of airgun noise received in Antarctica was slightly higher, when the sea depth at the source location varied within approximately 300-700 m, than that when the sea was deeper (800-1200 m).

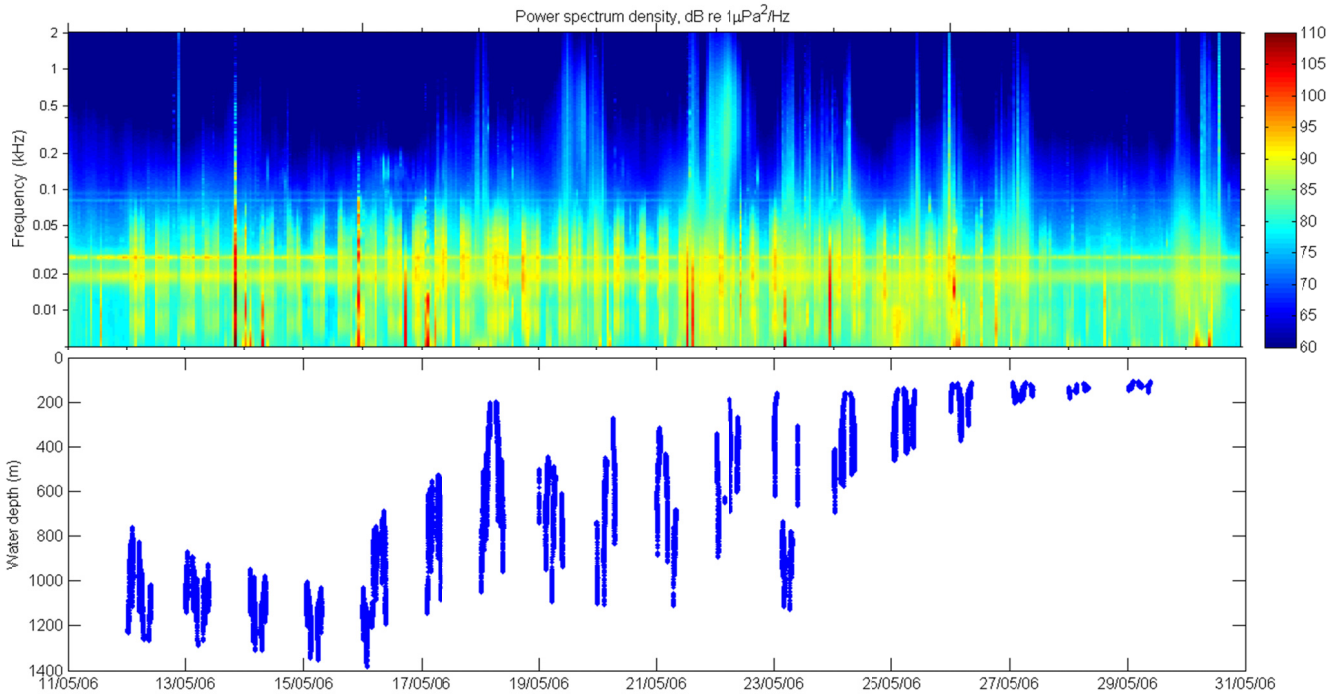

Figure 6: Long-time average spectrogram of sea noise recorded over the time period of the major part of the Aragorn seismic survey in May 2006 (top panel) and sea depth at the source location at the airgun discharge times (bottom panel).

Figure 7 shows the waveform (top) and spectrogram (bottom) of a 200-s section of the sea noise recording made on the 18th of May which contains the airgun noise of higher intensity. The sound exposure level (SEL) of the received airgun signals corrected for the intensity of background noise varied within 117.5-118 dB re 1 $\mu Pa^2 \cdot s$.

Figure 8 shows the transmission loss versus range and depth modelled at 10 Hz, 30 Hz and 100 Hz. In these figures, the transmission loss is compared for source locations 1, 3 and 5, where the sea depth at the source location was about 160 m, 360 m and 1160 m respectively. At 10 and 30 Hz, the effect of sound energy transmission from the deep SOFAR sound channel to the near-surface channel in the polar environment is clearly seen when the source is located in shallower water. This is not surprising as in shallow water more sound ener-

gy is distributed into low-order modes concentrated near the sound channel axis. Consequently, the sound level at the receiver placed near the bottom in Antarctica, far away from the sound channel axis, is lower.

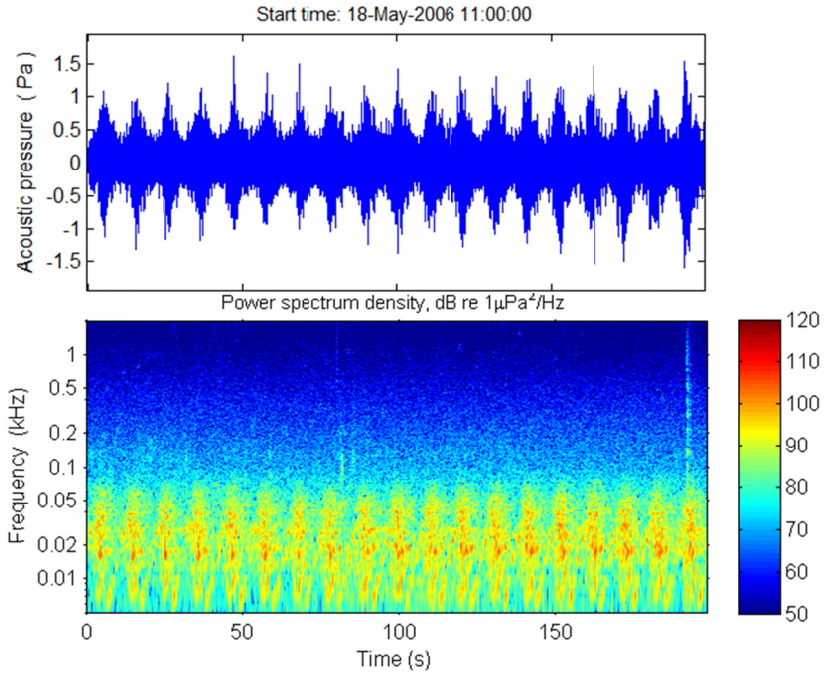

Figure 7: Impulsive airgun noise from the Aragorn seismic survey recorded on the 18th of May: waveform (top) and spectrogram (bottom).

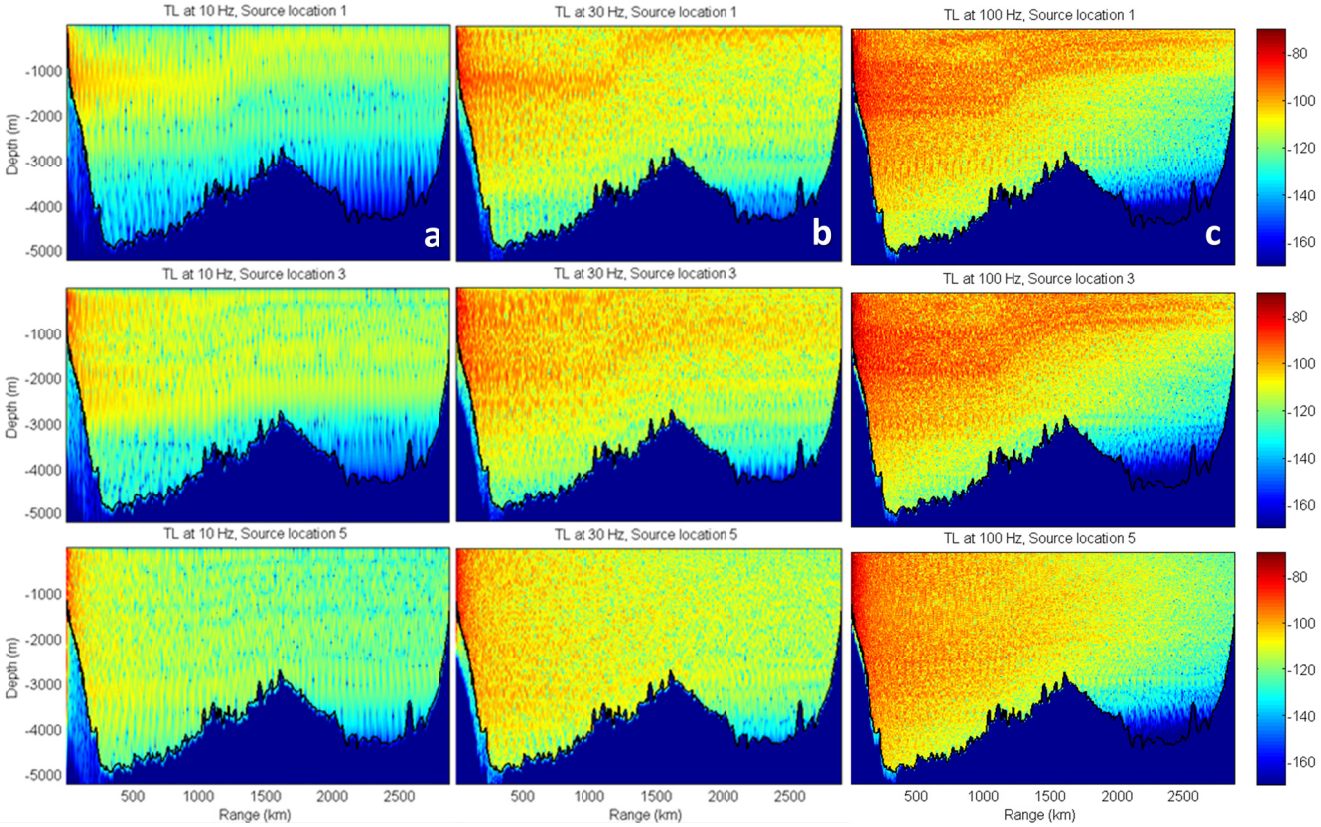

Figure 8: Transmission loss modelled at 10 Hz (a), 30 Hz (b) and 100 Hz (c) for source locations 1 (top row), 3 (middle row) and 5 (bottom row).

The transmission loss at the receiver is generally lower in this frequency band, when the sea depth at the source is moderate but less than the depth of the SOFAR channel axis. The maximum transmission loss at all frequencies occurs when the sound source is located in deep water where the sea depth is larger than 1000 m. In this case, a shallow source is not well coupled with the deep SOFAR channel through the interaction with the sloping seabed.

To illustrate the role of sea surface scattering in the sound transmission loss, Figure 9 shows the attenuation coefficient of mode 10 versus range and frequency. At low frequencies, modal attenuation results primarily from sound absorption in the seabed, whereas at higher frequencies it is governed by the sea surface scattering effect, which is obvious beyond the polar front from about 1500 km. Lower order modes are less sensitive to the surface scattering effect; however they do not contribute significantly to the sound field near the bottom.

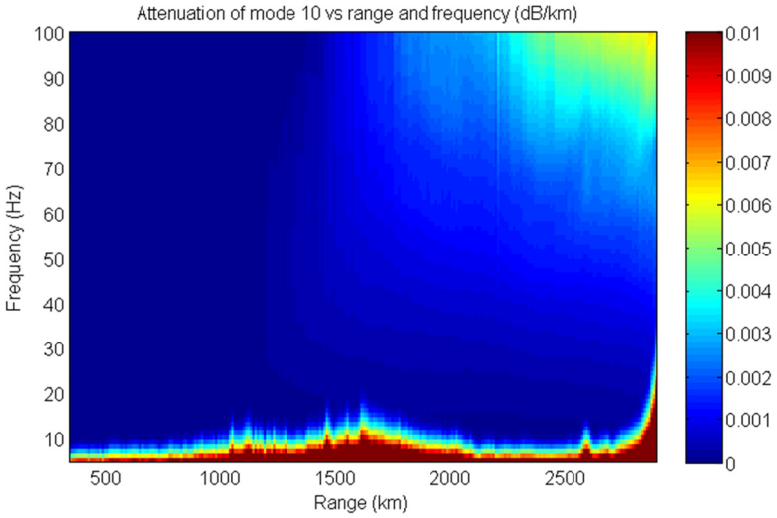

Figure 9: Attenuation coefficient of mode 10 vs range and frequency.

The ESD level ESD_R of the received signal was calculated from the ESD level ESD_S of the source signal and the transmission loss TL, as $ESD_R = ESD_S - TL$. The ESD level of the airgun array signal recorded on the 18th of May, when it was near the maximum value, is compared in Figure 10 with that predicted by numerical modelling for three different locations of the sound source. The agreement between the modelling and measurement results is good, especially for the source location at a sea depth of 360 m (source location 3).

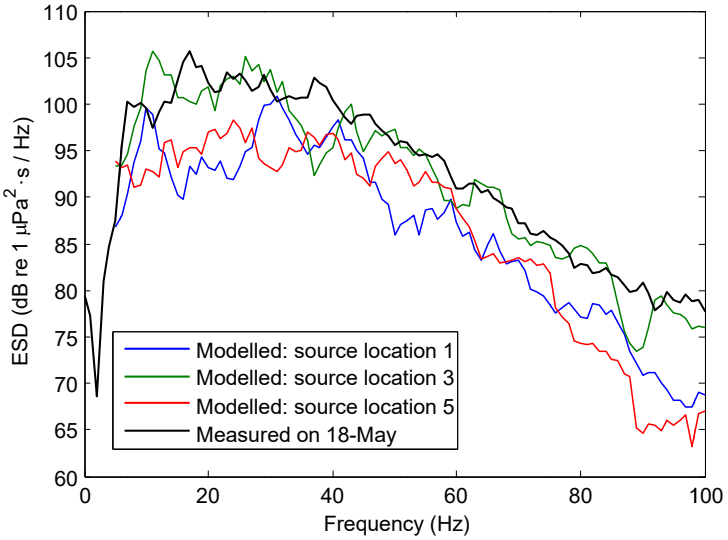

Figure 10: Modelled and measured energy spectral density levels of the received signals.

When comparing ESD_R (Figure 10) with ESD_S (Figure 3), one can conclude that the frequency dependence of the transmission loss is low. Indeed, the slope of ESD_R and ESD_S curves is similar between approximately 30 Hz and 80 Hz where the effects of bottom interaction and surface scattering are not significant compared to that

of spreading loss (Figure 8). At frequencies below approximately 30 Hz, the attenuation is noticeably higher due to interaction of low order modes with the seabed over the shallower section of the continental slope. At frequencies above approximately 80 Hz, the effect of surface scattering becomes significant in the transmission loss.

Finally, the SEL was calculated as a function of depth at the receiver location. Figure 11 shows the modelled SEL versus depth and the SEL value of the airgun signals measured on the 18th of May. The plot clearly demonstrates that the sound transmission from a shallow sound source over the continental slope is more efficient when the sea depth at the source location is smaller than the depth of the SOFAR channel axis. When the sea depth at the source location is 150-200 m, the sound energy at the receiver location tends to concentrate in the top 200-m water layer. As the sea depth at the source location increases, the SEL becomes more evenly distributed across the water column.

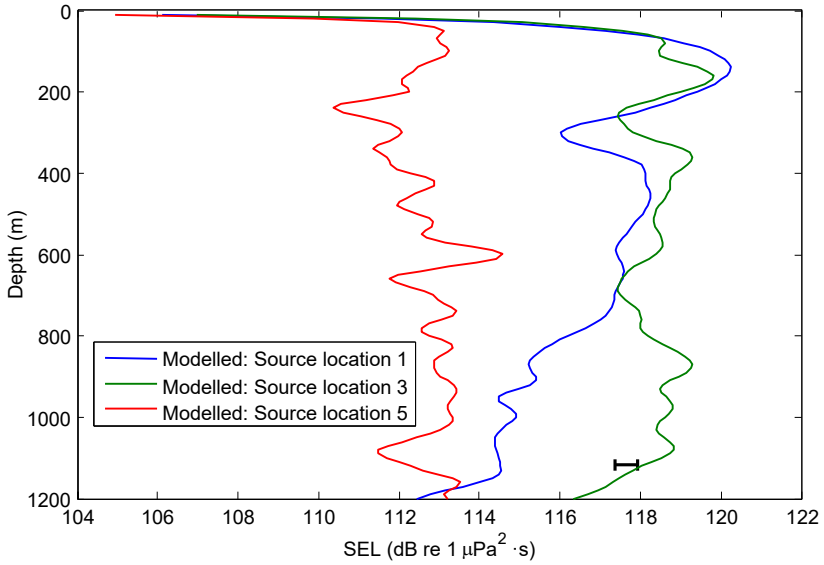

Figure 11: SEL of the received signal vs receiver depth at the distance to the sound recorder modelled for three sound source locations. The horizontal error bar shows the range of SEL variations measured on the 18th of May.

4 SUMMARY

The sound emission and propagation model employed in this numerical study resulted in a good agreement of the modelling results with the measurement data with respect to both ESD and SEL of the received signal. However, the modelling results were verified by measurements only for a receiver placed near the seabed. The comparison of the numerical predictions and measurement data would be much more comprehensive if we had measurements made at different (shallower) receiver depths.

It's also important to add that the measurements were made in austral summer when the Southern Ocean off Eastern Antarctica is free of sea ice. In such conditions the airgun sound trapped in the polar near-surface sound channel was affected by the transmission loss due to sound scattering from surface waves. A significant wave height of approximately 8 m typical for the Southern Ocean south of the Antarctic polar front was used in the sound transmission model, which resulted in a good agreement of modelling and measurement results. In austral winter, an extensive area of the Southern Ocean south of the East Antarctic coast is covered by sea ice, which affects the surface scattering mechanism and should be taken into consideration in the sound transmission model.

ACKNOWLEDGEMENTS

This modelling study was funded by the German Federal Ministry for the Environment, Nature Conservation, Building and Nuclear Safety (FKZ 3714 19 1010) under a contract with the Institute for Terrestrial and Aquatic Wildlife Research, University of Veterinary Medicine, Hannover. The authors also acknowledge the effort and experience of the AAD team led by Dr Jason Gedamke who deployed and retrieves the underwater sound recorders in the Southern Ocean.

REFERENCES

Duncan, A. 1998. “Research into the Acoustic Characteristics of an Air Gun Sound Source.” CMST Report C98-18 prepared for the Defence Science and Technology Organisation, Curtin University.

Gavrilov, A., McCauley, R.M., and Erbe, C. 2016. “Assessment of Potential Disturbance by Masking during Use of Airguns in Antarctica: Description of Raw Data (Recordings of Seismic Airguns and Ambient Noise) held at CMST.” CMST Report 2016-9 prepared for University of Hannover, Curtin University.

Kuperman, W.A., and Ingenito, F. 1977. “Attenuation of coherent component of sound propagating in shallow water with rough boundaries.” *J. Acoust. Soc. Am.* 61, 1178-1187.

Li, B., and Gavrilov, A.N. 2006. “Hydroacoustic Observation of Antarctic Ice Disintegration Events in the Indian Ocean.” *First Australasian Acoustical Societies' Conference, Acoustics 2006: Noise of Progress,* pp 479-484, Christchurch New Zealand, 20-22 November 2006;

Westwood, E., Tindle, C. T., and Chapman, N. R. 1996. “A normal mode model for acoustic-elastic ocean environments.” *J. Acoust. Soc. Am.* 100, 3631-3645.

Wilkes, D. R., Gourlay, T. P., and Gavrilov, A. N. 2016. “Numerical modeling of radiated sound for impact pile driving in offshore environments.” *IEEE J. Oceanic Eng.* 41, 1072-1078.